Hindawi
International Journal of Aerospace Engineering
Volume 2022, Article ID 1908020, 8 pages
https://doi.org/10.1155/2022/1908020

Research Article

Research on Aircraft Attitude Control Method Based on Linear Active Disturbance Rejection

Zhiguo Song,[1,2] **Changjian Zhao**,[2] **Huiqiang Zhang**,[1] **Tian Dong**,[2] **Aojia Ma**,[2] **and Dawei Yan**[2]

[1]*School of Aerospace Engineering, Tsinghua University, Beijing 100084, China*
[2]*China Academy of Launch Vehicle Technology, Beijing 100076, China*

Correspondence should be addressed to Zhiguo Song; szglvlm@163.com

Received 11 June 2022; Revised 24 July 2022; Accepted 26 July 2022; Published 17 August 2022

Academic Editor: Chuang Liu

In this paper, a dual-loop active disturbance rejection attitude controller design method is proposed for the attitude control of aircraft. Firstly, based on the nonlinear dynamic model of aircraft, the control system model with inner loop as angular velocity and outer loop as attitude angle is established. Secondly, the extended state observer for the inner loop is established to estimate and compensate the state of the system in real time. The controller of the compensated series integral system is designed by using the linear PD control method. Thirdly, the extended state observer and controller for the outer loop are designed by the same method. Finally, the stability proof of the dual-loop attitude control method is given based on the Lyapunov theorem of stability. Simulation results show that compared with the traditional PID attitude control method, the dual-loop ADRC attitude control method has better control quality in tracking speed, tracking error, and system anti-interference ability. The control parameters to be adjusted in this method have distinct physical significance. So this method has a wide range of engineering application prospects.

1. Introduction

Traditional aircraft attitude control system is usually based on small disturbance linearization theory [1]. The six degree of freedom dynamic equation is linearized with small perturbation near the standard trajectory, and the coupling effect between channels is ignored. Typical characteristic points are selected to change the time-varying system into a time invariant system. A single channel attitude control system is designed based on linear control theory. However, with the increasing demand for aircraft performance, high-speed booster aircraft appeared. This kind of aircraft adopts the shape of lift body and flies in the atmosphere with high maneuverability. It has the characteristics of large airspace, wide velocity domain, and high dynamic response. The aircraft has strong coupling, fast time-varying, and strong nonlinear characteristics among the three channels of pitch, yaw, and roll. The design method of attitude control system based on linear control theory is difficult to meet the requirements of maneuvering flight.

Modern control methods have been widely studied. Sliding mode control has strong robustness. Keke Shi et al. developed an improved finite time sliding mode control strategy to satisfy good orbit-attitude tracking performance [2]. Chintapalli Vaishnavi and M.V. Dhekane adopted H-infinity control method in autopilot design [3]. Active disturbance rejection control (ADRC) is a nonlinear adaptive control method proposed by Professor Jingqing Han [1]. In this method, the uncertainty and unmodeled error of the model are classified as "total disturbance" of the system [4]. The internal and external disturbances of the system can be estimated and compensated in real time. Based on the simple linear model, the disturbance is compensated and the control law is designed to obtain better

control quality. However, these methods use more nonlinear functions, which is not convenient for stability analysis and control parameter design. Zhiqiang Gao and other scholars linearized the main links of active disturbance rejection control and proposed a linear active disturbance rejection control method (LADRC) [5–10]. The design parameters of this method have clear physical meaning and are easy to be adjusted. It is suitable for engineering application.

Mingwei Sun, Sa Lin, etc. studied the attitude control of aircraft pitch channel based on active disturbance rejection control technology. The superiority of ADRC over traditional PD control method is verified. However, the research object is the linearized model of aircraft pitch channel, ignoring the nonlinear factors and the coupling between channels [11, 12]. Naigang Cui et al. designed an attitude controller based on ADRC for the three channel nonlinear model of reusable launch vehicle. The stable flight from active phase to reentry phase is realized, and the controller has good control effect. However, due to the use of nonlinear error feedback rate, too many parameters need to be designed and adjusted, and there is a lack of stability proof [13]. The ADRC scheme has been employed in other field [14–18]. Chuang Liu et al. develop an IO-based ADRC scheme without knowing exactly the external disturbances, fault signals, time-varying delay, and mass properties to achieve high-precision electromagnetic docking of spacecraft in elliptical orbits [14]. Linxing Xu applied a cascade ADRC scheme in the attitude subsystem of a quadrotor unmanned aerial vehicle [18].

Most scholars focus on broadening the application of ADRC technology and the adjustment method of control parameters, while a few scholars focus on the physical meaning of parameters and the proof method of stability. In this paper, the nonlinear dynamic model of aircraft is studied at first. Then, a dual-loop attitude control system model is established. On this basis, the linear extended state observers of inner loop and outer loop are established to observe and compensate the matching error and non-matching error, respectively. And the inner loop and outer loop controllers are designed based on the linear error feedback law. Additionally, the parameters are adjusted according to the physical meaning of the control parameters. Finally, the stability proof is given based on the Lyapunov theorem of stability. Simulation results validate the effectiveness of the proposed approach and the improved performance comparing to the traditional autopilot without lateral thrusters.

2. Nonlinear Model of General Aircraft

The force required for the movement of the aircraft is aerodynamic force, which is caused by the deflection of the air vane. Define the motion around the X axis of the body coordinate system as rolling, the motion around the Y axis as yaw, and the motion around the Z axis as pitch. According to the theorem of momentum, the motion around the center of mass is described in the body coordinate system. The nonlinear mathematical model of the aircraft's motion around the center is established as follows.

$$\begin{bmatrix}\dot{\omega}_{x1}\\ \dot{\omega}_{y1}\\ \dot{\omega}_{z1}\end{bmatrix} = \begin{bmatrix}\frac{J_{y1}-J_{z1}}{J_{x1}}\omega_{y1}\omega_{z1}\\ \frac{J_{z1}-J_{x1}}{J_{y1}}\omega_{z1}\omega_{x1}\\ \frac{J_{x1}-J_{y1}}{J_{z1}}\omega_{x1}\omega_{y1}\end{bmatrix} + \begin{bmatrix}\frac{M_{px1}}{J_{x1}}\\ \frac{M_{py1}}{J_{y1}}\\ \frac{M_{pz1}}{J_{z1}}\end{bmatrix} + \begin{bmatrix}\frac{M_{dx1}}{J_{x1}}\\ \frac{M_{dy1}}{J_{y1}}\\ \frac{M_{dz1}}{J_{z1}}\end{bmatrix} + \begin{bmatrix}\frac{C^{\delta_0}_{mx1}qS_mL_k}{J_{x1}}\\ \frac{C^{\delta_0}_{my1}qS_mL_k}{J_{y1}}\\ \frac{C^{\delta_0}_{mz1}qS_mL_k}{J_{z1}}\end{bmatrix} + \begin{bmatrix}\frac{C^{\delta_\gamma}_{mx1}qS_mL_k}{J_{x1}} & \frac{C^{\delta_\psi}_{mx1}qS_mL_k}{J_{x1}} & \frac{C^{\delta_\varphi}_{mx1}qS_mL_k}{J_{x1}}\\ \frac{C^{\delta_\gamma}_{my1}qS_mL_k}{J_{y1}} & \frac{C^{\delta_\psi}_{my1}qS_mL_k}{J_{y1}} & \frac{C^{\delta_\varphi}_{my1}qS_mL_k}{J_{y1}}\\ \frac{C^{\delta_\gamma}_{mz1}qS_mL_k}{J_{z1}} & \frac{C^{\delta_\psi}_{mz1}qS_mL_k}{J_{z1}} & \frac{C^{\delta_\varphi}_{mz1}qS_mL_k}{J_{z1}}\end{bmatrix}\begin{bmatrix}\delta_\gamma\\ \delta_\psi\\ \delta_\varphi\end{bmatrix}, \tag{1}$$

$$\begin{bmatrix}\dot{\gamma}\\ \dot{\psi}\\ \dot{\phi}\end{bmatrix} = \begin{bmatrix}1 & \sin\gamma\mathrm{tg}\psi & \cos\gamma\mathrm{tg}\psi\\ 0 & \cos\gamma & -\sin\gamma\\ 0 & \sin\gamma/\cos\psi & \cos\gamma/\cos\psi\end{bmatrix}\begin{bmatrix}\omega_{x1}\\ \omega_{y1}\\ \omega_{z1}\end{bmatrix}, \tag{2}$$

Sort the above formula as:

$$\dot{\omega} = f_1(\cdot) + g_1\delta, \tag{3}$$

$$\dot{\Omega} = g_2\omega, \tag{4}$$

with,

$$f_1(\cdot) = \begin{bmatrix}\frac{J_{y1}-J_{z1}}{J_{x1}}\omega_{y1}\omega_{z1}\\ \frac{J_{z1}-J_{x1}}{J_{y1}}\omega_{z1}\omega_{x1}\\ \frac{J_{x1}-J_{y1}}{J_{z1}}\omega_{x1}\omega_{y1}\end{bmatrix} + \begin{bmatrix}\frac{M_{px1}}{J_{x1}}\\ \frac{M_{py1}}{J_{y1}}\\ \frac{M_{pz1}}{J_{z1}}\end{bmatrix} + \begin{bmatrix}\frac{M_{dx1}}{J_{x1}}\\ \frac{M_{dy1}}{J_{y1}}\\ \frac{M_{dz1}}{J_{z1}}\end{bmatrix} + \begin{bmatrix}\frac{C^{\delta_0}_{mx1}qS_mL_k}{J_{x1}}\\ \frac{C^{\delta_0}_{my1}qS_mL_k}{J_{y1}}\\ \frac{C^{\delta_0}_{mz1}qS_mL_k}{J_{z1}}\end{bmatrix}, \tag{5}$$

$$g_1 = \begin{bmatrix}\frac{C^{\delta_\gamma}_{mx1}qS_mL_k}{J_{x1}} & \frac{C^{\delta_\psi}_{mx1}qS_mL_k}{J_{x1}} & \frac{C^{\delta_\varphi}_{mx1}qS_mL_k}{J_{x1}}\\ \frac{C^{\delta_\gamma}_{my1}qS_mL_k}{J_{y1}} & \frac{C^{\delta_\psi}_{my1}qS_mL_k}{J_{y1}} & \frac{C^{\delta_\varphi}_{my1}qS_mL_k}{J_{y1}}\\ \frac{C^{\delta_\gamma}_{mz1}qS_mL_k}{J_{z1}} & \frac{C^{\delta_\psi}_{mz1}qS_mL_k}{J_{z1}} & \frac{C^{\delta_\varphi}_{mz1}qS_mL_k}{J_{z1}}\end{bmatrix}, \tag{6}$$

$$g_2 = \begin{bmatrix}1 & \sin\gamma\mathrm{tg}\psi & \cos\gamma\mathrm{tg}\psi\\ 0 & \cos\gamma & -\sin\gamma\\ 0 & \sin\gamma/\cos\psi & \cos\gamma/\cos\psi\end{bmatrix}, \tag{7}$$

where $\omega = [\omega_{x1}\omega_{y1}\omega_{z1}]^T$ are angular velocity components observed in the body coordinate system. $\Omega = [\gamma\ \psi\ \varphi]^T$ are three attitude angles. $\delta = \begin{bmatrix}\delta_\gamma & \delta_\psi & \delta_\varphi\end{bmatrix}^T$ are the deflection angles of aileron, rudder, and elevator. $\begin{bmatrix}M_{px1} & M_{py1} & M_{pz1}\end{bmatrix}^T$ are components of engine thrust in three directions of body coordinate system. $\begin{bmatrix}M_{dx1} & M_{dy1} & M_{dz1}\end{bmatrix}^T$ are components of disturbance in three directions of body coordinate system. $\begin{bmatrix}C_{mx1}^{\delta_0} & C_{my1}^{\delta_0} & C_{mz1}^{\delta_0}\end{bmatrix}^T$ are the coefficients of the aerodynamic moment when aileron, rudder, and elevator deflection angles are zero. $C_{mi1}^{\delta_j}, (i = x, y, z\,; j = \gamma, \psi, \varphi)$ is the partial derivative of aerodynamic moment coefficient to aerodynamic rudder deflection angle. $f_1(\cdot)$ includes the system unmodeled dynamics, external interference, and other uncertainties. g_1, g_2 are accurate known term.

Based on the above nonlinear model, Equation (3) is the inner loop as angular velocity and Equation (4) is the outer loop as attitude angle. For each loop, a linear extended state observer is established to estimate and compensate the state of the system in real time, and a PD linear error feedback control law is designed to realize the attitude control of the aircraft.

3. Linear Active Disturbance Rejection Control

LADRC is a nonlinear control method which has great robustness against the model parameter variation and disturbance [19, 20]. The n-order nonlinear SISO system is considered as follows.

$$y^n(t) = f\left(y^{(n-1)}(t), y^{(n-2)}(t), \cdots, y(t), w(t)\right) + bu(t), \quad (8)$$

where $w(t)$ is the external disturbance, b is the given constant, and $f(y^{(n-1)}(t), y^{(n-2)}(t), \cdots, y(t), w(t))$ can be simply calculated as f, representing the nonlinear dynamics with unmodeled disturbance. Only the order and b are known. Assuming that f is differentiable and let $h = \dot{f}$, the above formula can be written in the form of state space, as

$$\begin{cases} \dot{x}_1 = x_2 \\ \quad\vdots \\ \dot{x}_{n-1} = x_n \\ \dot{x}_n = x_{n+1} + bu \\ \dot{x}_{n+1} = h(x, w) \\ y = x_1 \end{cases}, \quad (9)$$

where $x_{n+1} = f(y^{(n-1)}(t), y^{(n-2)}(t), \cdots, y(t), w(t))$ is the expanded state of the system.

3.1. Linear Extended State Observer. The linear extended state observer (LESO) is constructed as follows.

$$\begin{cases} \dot{\hat{x}}_1 = \hat{x}_2 + l_1(x_1 - \hat{x}_1) \\ \quad\vdots \\ \dot{\hat{x}}_{n-1} = \hat{x}_n + l_{n-1}(x_1 - \hat{x}_1) \\ \dot{\hat{x}}_n = \hat{x}_{n+1} + l_n(x_1 - \hat{x}_1) + b_0 u \\ \dot{\hat{x}}_{n+1} = l_{n+1}(x_1 - \hat{x}_1) \end{cases}, \quad (10)$$

where $l_i, i = 1, 2, \cdots n+1$ is the observer gain parameter. b_0 is the estimated value of control gain b. The observer gain parameters are selected as follows.

$$\begin{bmatrix} l_1 & l_2 & \cdots & l_{n+1}\end{bmatrix} = \begin{bmatrix}\omega_0\alpha_1 & \omega_0^2\alpha_2 & \cdots & \omega_0^{n+1}\alpha_{n+1}\end{bmatrix}$$
$$\alpha_i = \frac{(n+1)!}{i!(n+1-i)!}. \quad (11)$$

Then, the LESO can be configured as

$$\lambda_0(s) = s^{n+1} + \omega_0\alpha_1 s^n + \cdots + \omega_0^n\alpha_n s + \omega_0^{n+1}\alpha_{n+!} = (s + \omega_0)^n, \quad (12)$$

where ω_0 is bandwidth of the LESO.

3.2. Linear Error Feedback Law. When LESO observes the total disturbance of the system in real time, we can get the observed expansion state as

$$\hat{x}_{n+1} \approx x_{n+1} = f\left(y^{(n-1)}(t), y^{(n-2)}(t), \cdots, y(t), w(t)\right). \quad (13)$$

Select the following control quantities:

$$u = \frac{u_0 - \hat{x}_{n+1}}{b_0}, \quad (14)$$

where u_0 is the virtual control quantity. Substituting u into Equation (8), the system becomes a series integral system, as

$$y^n(t) = (f - \hat{x}_{n+1}) + u_0 \approx u_0. \quad (15)$$

The virtual control quantity u_0 takes the form of proportion and higher-order differential as

$$u_0 = k_p(r_1 - \hat{x}_1) + k_{d_1}\hat{x}_2 \cdots + k_{d_{n-1}}\hat{x}_n. \quad (16)$$

If $k_p, k_{d_1}, \cdots k_{d_{n-1}}$ are the coefficients of the closed-loop characteristic polynomial of the system, the closed-loop system can be configured as the following characteristic polynomial.

$$\lambda_c(s) = s^n + k_{d_{n-1}}s^{n-1} + \cdots + k_{d_1}s + k_p = (s + \omega_c)^n, \quad (17)$$

where ω_c is the bandwidth of the controller example.

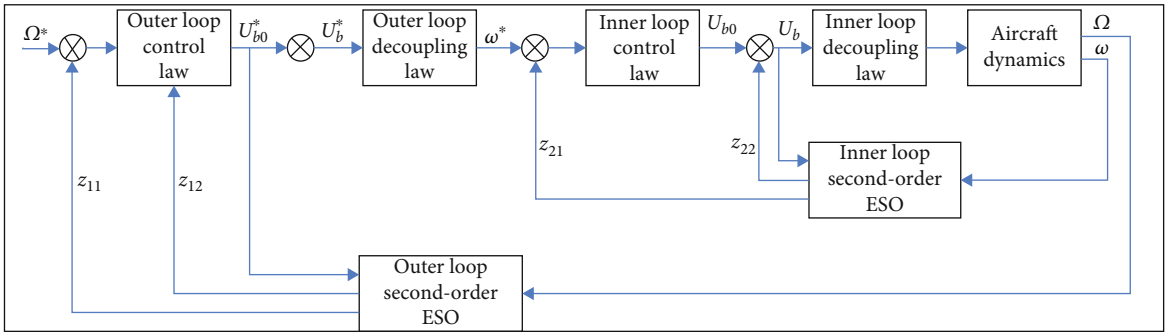

Figure 1: The diagram of a dual-loop attitude controller based on LADRC.

Reasonably select observer bandwidth and controller bandwidth, and $\omega_0 > 0, \omega_c > 0, \omega_0 > 5\omega_c$ is ensured. Then, the state estimation of the system and the stability control of the nonlinear system can be realized.

3.3. Attitude Control System Design. A dual-loop attitude controller based on ADRC is designed with the following structure in Figure 1

The pitching, yaw, and rolling channels of the aircraft adopt the double loop controller shown in Figure 1. The extended state observer and controller for the inner loop are designed at first. When the inner loop response is fast enough, it can be approximated as a straight loop. Then, a controller with the same structure is designed for the outer loop to realize attitude control.

3.4. Design of Inner Loop Controller. The inner loop corresponds to Equation (3), which is rewritten as

$$\dot{\omega} = f_1(\cdot) + U_b, \tag{18}$$

with,

$$U_b = g_1 \delta. \tag{19}$$

Construct LESO in three channels. The LESO is shown as follows.

$$\begin{aligned} e_{20} &= z_{21} - \omega, \\ \dot{z}_{21} &= z_{22} - l_{21} e_{20} + U_b, \\ \dot{z}_{22} &= -l_{22} e_{20}, \end{aligned} \tag{20}$$

where $l_{21} > 0, l_{22} > 0$ is the gain of linear extended state observer. When the gain of the extended state observer is reasonably selected, the following convergence results will be obtained when it reaches stability.

$$\begin{aligned} z_{21} &\longrightarrow \omega, \\ z_{22} &\longrightarrow f_1(\cdot). \end{aligned} \tag{21}$$

The output of the extended state observer can estimate the attitude angular velocity. And on the other hand, it can estimate the total "disturbance" of the unmodeled dynamics and uncertain disturbances of the system. According to the principle of linear extended state observer, the observer gain is selected as

$$\begin{bmatrix} l_{21} & l_{22} \end{bmatrix} = \begin{bmatrix} 2\omega_{02} & \omega_{02}^2 \end{bmatrix}. \tag{22}$$

Then, the LESO can be configured as

$$\lambda_0(s) = s^2 + 2\omega_{02} s + \omega_{02}^2 = (s + \omega_{02})^2. \tag{23}$$

The virtual control quantity is designed as

$$U_b = U_{b0} - z_{22}. \tag{24}$$

Substitute Equation (24) into Equation (18), we can get

$$\dot{\omega} = U_{b0}. \tag{25}$$

Adopting PD linear error feedback control law, the virtual control can be obtained as

$$\begin{aligned} e_2 &= \omega^* - z_{21}, \\ U_{b0} &= k_{p2} e_2 + k_{d2} \dot{e}_2. \end{aligned} \tag{26}$$

The gain of linear error feedback law is selected as

$$\begin{bmatrix} k_{d2} & k_{p2} \end{bmatrix} = \begin{bmatrix} 2\omega_{c2} & \omega_{c2}^2 \end{bmatrix}. \tag{27}$$

So, the system can be configured as follows.

$$\lambda_c(s) = s^2 + 2\omega_{c2} s + \omega_{c2}^2 = (s + \omega_{c2})^2. \tag{28}$$

In order to obtain aerodynamic rudder deflection angles of three channels, the following decoupling control law is adopted

$$\delta = g_1^{-1} U_b. \tag{29}$$

By properly selecting ω_{02} and ω_{c2}, the inner loop attitude angular velocity control can be realized.

3.5. Design of Outer Loop Controller. The outer loop corresponds to Equation (4), which is rewritten as

$$\dot{\Omega} = U_b^*. \tag{30}$$

with,

$$U_b^* = g_2\omega. \tag{31}$$

A LESO with the same structure as inner loop is designed as follows.

$$\begin{aligned} e_{10} &= z_{11} - \Omega, \\ \dot{z}_{11} &= z_{12} - l_{11}e_{10} + U_b^*, \\ \dot{z}_{12} &= -l_{12}e_{10}, \end{aligned} \tag{32}$$

where $l_{11} > 0, l_{12} > 0$ are the gains of LESO. When the gains are chosen properly, the observer can converge stably. The observer parameters are taken as follows.

$$\begin{bmatrix} l_{11} & l_{12} \end{bmatrix} = \begin{bmatrix} 2\omega_{01} & \omega_{01}^2 \end{bmatrix}. \tag{33}$$

The outer loop LESO can be configured as

$$\lambda_0(s) = s^2 + 2\omega_{01}s + \omega_{01}^2 = (s + \omega_{01})^2. \tag{34}$$

Equation (30) is a single integral system. Similarly, PD linear error feedback control law is selected. The virtual control quantity can be obtained as

$$\begin{aligned} e_1 &= \Omega^* - z_{11}, \\ U_{b0}^* &= k_{p1}e_1 + k_{d1}\dot{e}_1. \end{aligned} \tag{35}$$

The gain of outer loop linear error feedback law is selected as

$$\begin{bmatrix} k_{d1} & k_{p1} \end{bmatrix} = \begin{bmatrix} 2\omega_{c1} & \omega_{c1}^2 \end{bmatrix}. \tag{36}$$

The system can be configured as

$$\lambda_c(s) = s^2 + 2\omega_{c1}s + \omega_{c1}^2 = (s + \omega_{c1})^2. \tag{37}$$

The desired attitude angular velocity of three channels can be obtained by selecting the following decoupling control law.

$$\omega^* = g_2^{-1}U_b^*. \tag{38}$$

By properly selecting ω_{01} and ω_{c1}, the outer loop attitude angle control can be realized.

3.6. Stability Analysis. Taking the inner loop angular velocity control as an example, the stability analysis is carried out. Abbreviate Equation (18) as $\dot{\omega} = f + bu$ and take $x_1 = \omega, x_2 = f$, then the system can be rewritten as

$$\begin{aligned} \dot{x} &= Ax + Bu + Eh, \\ y &= Cx, \end{aligned} \tag{39}$$

with,

$$A = \begin{bmatrix} 0 & 1 \\ 0 & 0 \end{bmatrix}, B = \begin{bmatrix} b \\ 0 \end{bmatrix}, E = \begin{bmatrix} 0 \\ 1 \end{bmatrix}, C = \begin{bmatrix} 1 & 0 \end{bmatrix}, \tag{40}$$

where $h = \dot{f}$. f is differentiable.

Take $z = \begin{bmatrix} z_{21} & z_{22} \end{bmatrix}^T$ and $L = \begin{bmatrix} l_{21} & l_{22} \end{bmatrix}^T$, the LESO is obtained as

$$\begin{aligned} \dot{z} &= Az + Bu + L(y - \hat{y}), \\ \hat{y} &= Cz. \end{aligned} \tag{41}$$

Define the observation error as $e = x - z$, then the following can be obtained from Equation (39) and Equation (41).

$$\dot{e} = A_e e + d, \tag{42}$$

with,

$$A_e = A - LC = \begin{bmatrix} -l_{21} & 1 \\ -l_{22} & 0 \end{bmatrix}, d = Eh. \tag{43}$$

Design l_{21}, l_{22} so that A_e is a Hurwitz matrix and select Lyapunov function $V = e^T Pe$, where P is a positive definite matrix and satisfies Lyapunov equation.

$$A_e^T P + PA_e = -Q, \tag{44}$$

where Q is any positive definite matrix, then we can get

$$\begin{aligned} \dot{V} &= \dot{e}^T Pe + e^T P\dot{e} = (A_e e + d)^T Pe + e^T P(A_e e + d) \\ &= e^T\left(A_e^T P + PA_e\right)e + d^T Pe + e^T Pd = -e^T Qe + 2d^T Pe \\ &= -\left(e^T Q_2^1 - d^T PQ^{-\frac{1}{2}}\right)\left(e^T Q_2^1 - d^T PQ^{-\frac{1}{2}}\right)^T \\ &\quad + \left(d^T PQ^{-\frac{1}{2}}\right)\left(d^T PQ^{-\frac{1}{2}}\right)^T. \end{aligned} \tag{45}$$

Obviously, when $\|e^T Q_2^1 - d^T PQ^{-\frac{1}{2}}\|_2 > \|d^T PQ^{-\frac{1}{2}}\|_2$, $\dot{V} < 0$. Furthermore, when $\|e^T Q_2^1\|_2 > 2\|d^T PQ^{-\frac{1}{2}}\|_2$, $\dot{V} < 0$. When Q is an identity matrix, if $\|e\|_2 > 2\|Pd\|_2$, $\dot{V} < 0$. So e is bounded, and the boundary is $\|e\|_2 \le 2\|Pd\|_2$.

The above results can be further generalized as follows.

Lemma 1. For dynamic systems as $\dot{\xi} = M\xi + g(\xi)$. If M is a Hurwitz matrix, and $g(\xi)$ is bounded, ξ is bounded [7]. *On this basis, for the control system adopting the LESO of Equation (20) and the linear error feedback control law of Equation (26), the following closed-loop dynamics can be obtained.*

$$\begin{aligned} \dot{\omega} = f_1(\cdot) + U_b &= f_1(\cdot) + U_{b0} - z_{22} = f_1(\cdot) \\ &\quad - z_{22} + k_{p2}(\omega^* - z_{21}) + k_{d2}(\dot{\omega}^* - \dot{z}_{21}). \end{aligned} \tag{46}$$

Table 1: Aircraft parameter.

Parameters	Numerical value
M	19000 kg
J_{x1}	3900 kg.m^2
J_{y1}	393600 kg.m^2
J_{z1}	393600 kg.m^2
q	39900 pa
L_k	19 m
S_m	1.1 m^2
γ_0	3°
ψ_0	3°
φ_0	62°
ω_{x1_0}	0°
ω_{y1_0}	0°
ω_{z1_0}	0°
γ_c	0°
ψ_c	0°
φ_c	65°
ω_{x1_c}	0°
ω_{y1_c}	0°
ω_{z1_c}	0°

Sort Equation (47) as

$$\dot{\omega} = -k_{p2}\omega + \begin{bmatrix} k_{p2}k_{p2}k_{d2}k_{d2}1 \end{bmatrix} \begin{bmatrix} \omega^* \\ \omega - z_{21} \\ \dot{\omega}^* \\ \dot{\omega} - \dot{z}_{21} \\ f_1(\cdot) - z_{22} \end{bmatrix}, \quad (47)$$

where $-k_p$ makes the characteristic polynomial $s - k_p$ satisfy the Routh criterion, so $-k_p$ is Hurwitz stable. Meanwhile, ω^* and $\dot{\omega}^*$ are the bounded attitude angular velocity and attitude angular velocity integral command. $\omega - z_{21}$, $\dot{\omega} - \dot{z}_{21}$, and $f_1(\cdot) - z_{22}$ are the LESO estimation errors which are bounded based on Equation (45). Then, $[\omega^* \quad \omega - z_{21} \quad \dot{\omega}^* \quad \dot{\omega} - \dot{z}_{21} \quad f_1(\cdot) - z_{22}]^T$ are bounded. So ω is bounded according to Lemma 1. According to the definition of Lyapunov's stableness, the inner loop attitude angular velocity linear active disturbance rejection controller is stable. Similarly, it can be proved that the outer loop attitude angle linear ADRC is also stable.

3.7. Simulations and Analysis. In order to verify the attitude controller design method proposed in this paper, typical aircraft parameters are selected for simulation verification. Typical characteristic point parameters of aircraft are as follows (see Table 1).

Table 2: Control parameter.

Parameters	Numerical value
ω_{02}	200
ω_{c2}	10
ω_{01}	5
ω_{c1}	2

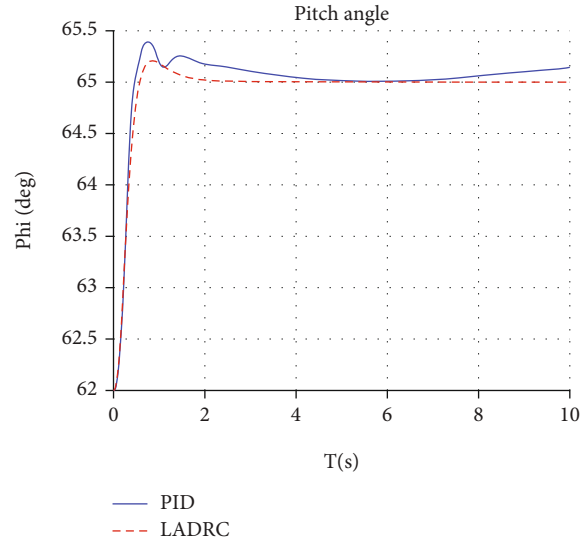

Figure 2: Variation of pitch angle.

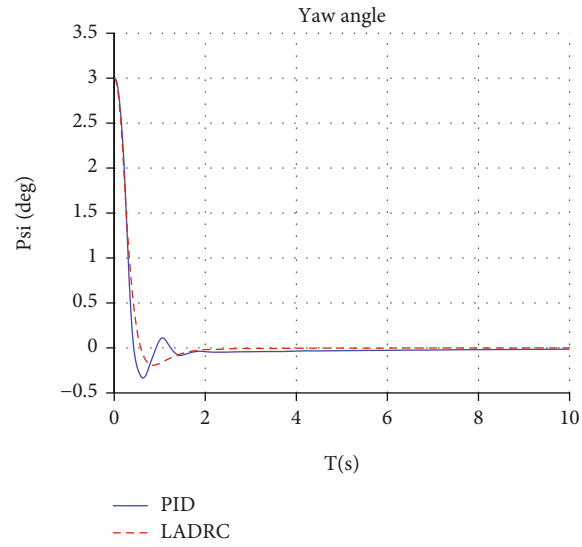

Figure 3: Variation of yaw angle.

The controller design method proposed in this paper needs less parameter to be adjusted. Only observer bandwidth and controller bandwidth need to be designed. The pitch, yaw, and roll channels use the same observer parameters and controller parameters. Specific control parameters are shown in Table 2.

Figures 2–4 show the comparison between the controller design method proposed in this paper and the traditional

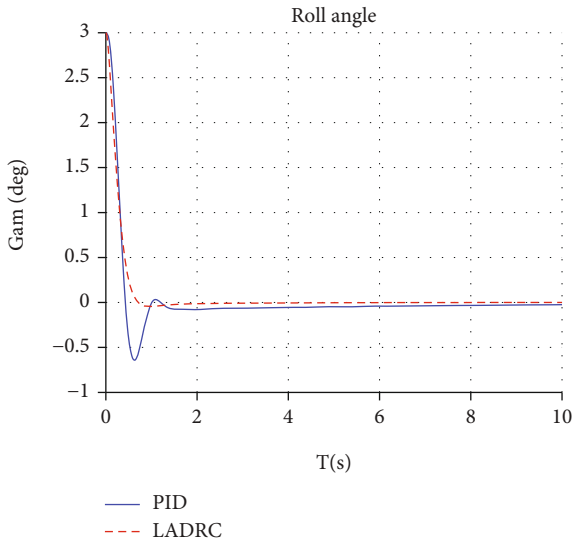

Figure 4: Variation of roll angle.

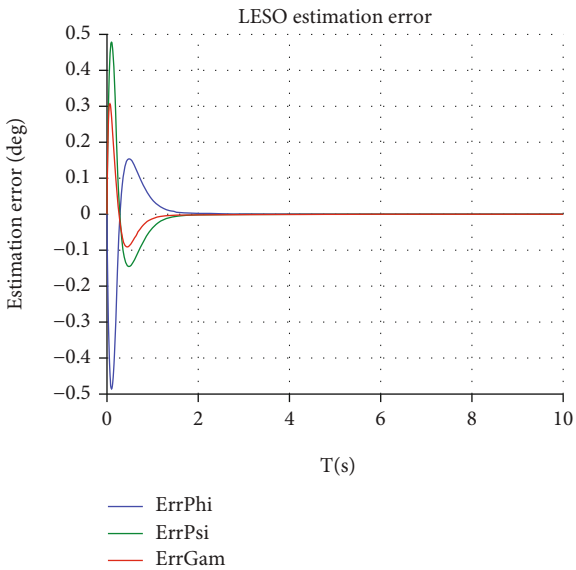

Figure 5: LESO attitude angle estimation error.

PID controller in the attitude angle tracking effect. The variation of pitch, yaw, and roll angle is smaller under LADRC. And the overshoot of LADRC control is less than 50% of that of traditional PID control. And the time to steady state is shorter under LADRC. Figures 5 and 6 show LESO estimation errors of attitude angle and attitude angular velocity, respectively. The estimation errors in all three channels converge quickly. From the above simulation results, it can be seen that the attitude controller based on LADR control has excellent control quality. Compared with the traditional PID control method, the designed controller can achieve rapid attitude stability of the aircraft, with small overshoot and steady-state error. The estimation performance of LESO is excellent and the estimation error can converge quickly.

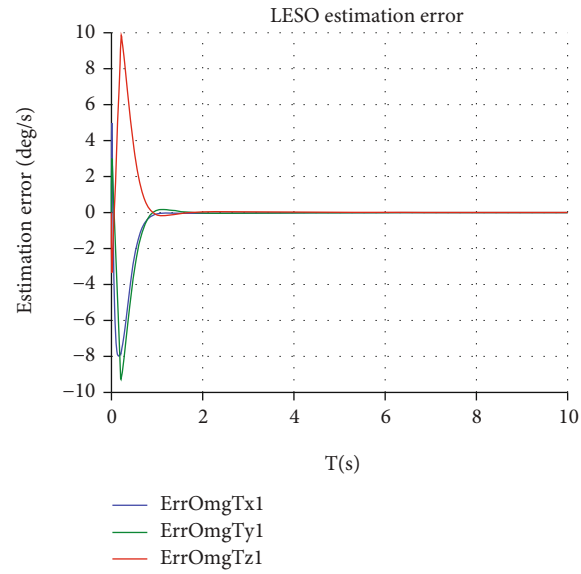

Figure 6: LESO attitude angle velocity estimation error.

4. Conclusions

In this paper, an attitude control method based on linear active disturbance rejection is proposed for the nonlinear model of aircraft. A dual loop linear extended state observer and linear error feedback control law are constructed. The stability of the proposed method is guaranteed. Simulation results show that the controller can achieve excellent performance only by reasonably designing the observer bandwidth and controller bandwidth. This method has clear physical meaning and strong practicability. Furthermore, the adaptability of this method to aircrafts used other actuators needs to be analyzed. And the influence of controller bandwidth and observer bandwidth on the controller effect should be analyzed theoretically from the perspective of stability principle.

Data Availability

The data used to support the findings of this study are available from the corresponding author upon request.

Conflicts of Interest

The authors declare that there is no conflict of interest regarding the publication of this paper.

References

[1] J. Han, "From PID to active disturbance rejection control," *IEEE Transactions on Industrial Electronics*, vol. 56, no. 3, pp. 900–906, 2009.

[2] K. Shi, C. Liu, Z. Sun, and X. Yue, "Coupled orbit-attitude dynamics and trajectory tracking control for spacecraft electromagnetic docking," *Applied Mathematical Modelling*, vol. 101, pp. 553–572, 2022.

[3] C. Vaishnavi and M. V. Dhekane, "Launch vehicle autopilot design using H-infinity control technique," *Communication and Control for Robotic Systems*, vol. 229, pp. 421–436, 2022.

[4] K. He, C. Dong, and Q. Wang, "active disturbance rejection control for uncertain nonlinear systems with sporadic measurements," *IEEE/CAA Journal of Automatica Sinica*, vol. 9, no. 5, pp. 893–906, 2022.

[5] Z. Gao, "Scaling and bandwidth-parameterization based controller tuning," in *Proceedings of the 2003 American Control Conference*, pp. 4989–4996, Denver, CO, USA, 2003.

[6] Q. Zheng, L. Q. Gao, and Z. Gao, "On validation of extended state observer through analysis and experimentation," *Journal of Dynamic Systems, Measurement, and Control*, vol. 134, no. 2, article 024505, 2012.

[7] Q. Zheng, L. Q. Gaol, and Z. Gao, "On stability analysis of active disturbance rejection control for nonlinear time-varying plants with unknown dynamics," in *2007 46th IEEE conference on decision and control*, pp. 3501–3506, New Orleans, LA, USA, 2007.

[8] Z. Gao, M. Sun, and R. Yang, "On the stability of l-inear active disturbance rejection control," *Acta Automatica Sinica*, vol. 39, no. 5, pp. 574–580, 2013.

[9] Q. Zheng, L. Dong, D. H. Lee, and Z. Gao, "Active disturbance rejection control for MEMS gyroscopes," *IEEE Transactions on Control Systems Technology*, vol. 17, no. 6, pp. 1432–1438, 2009.

[10] S. Zhao and Z. Gao, "Active disturbance rejection control. For non-minimum phase systems," in *Proceedings of the 29th Chinese control conference*, pp. 6066–6070, Beijing, China, 2010.

[11] M. Sun, R. Yang, and Z. Chen, "Flight Active Disturbance Rejection Control design and performance analysis," in *2010 8th World Congress on Intelligent Control and Automation*, pp. 765–770, Jinan, China, 2010.

[12] S. Lin, H. Lee, and W. Wu, "Design on attitude control based on linear ADRC for weapon in attack with high angle," *Tactical Missile Technology*, vol. 3, pp. 76–79, 2013.

[13] N. Cui, L. Zhang, C. Wei, and P. Han, "Active disturbance rejection control for reusable launch vehicle with large attitude maneuver," *Journal of Chinese Inertial Technology*, vol. 3, pp. 387–394, 2017.

[14] C. Liu, X. Yue, J. Zhang, and K. Shi, "Active disturbance rejection control for delayed electromagnetic docking of spacecraft in elliptical orbits," *IEEE Transactions on Aerospace and Elactronic Systems*, vol. 58, no. 3, pp. 2257–2268, 2022.

[15] Y. Yuan, Z. Wang, Y. Yu, L. Guo, and H. Yang, "Active disturbance rejection control for a pneumatic motion platform subject to actuator saturation: an extended state observer approach," *Automatica*, vol. 107, pp. 353–361, 2019.

[16] H. Yang, L. Cheng, Y. Xia, and Y. Yuan, "Active disturbance rejection attitude control for a dual closed-loop quadrotor under gust wind," *IEEE Transactions on Control Systems Technology*, vol. 26, no. 4, pp. 1400–1405, 2018.

[17] H. He and H. Duan, "A multi-strategy pigeon-inspired optimization approach to active disturbance rejection control parameters tuning for vertical take-off and landing fixed- wing UAV," *Chinese Journal of Aeronautics*, vol. 35, no. 1, pp. 19–30, 2022.

[18] X. Linxing, H. Ma, D. Guo, A. Xie, and D. Song, "Backstepping sliding-mode and cascade active disturbance rejection control for a quadrotor UAV," *IEEE/ASME Transactions on Mechatronics*, vol. 25, no. 6, pp. 2743–2753, 2020.

[19] Y. Huang and W. Xue, "Active disturbance rejection control: methodology and theoretical analysis," *ISA Transaction*, vol. 53, no. 4, pp. 963–976, 2014.

[20] Z. Gao, "Active disturbance rejection control: a paradigm shift in feedback control system design," in *2006 American Control Conference*, pp. 2399–2405, Minneapolis, MN, USA, 2006.